^{1}H-NMR and charge transport in metallic polypyrrole at ultra-low temperatures and high magnetic fields

2008 J. Phys.: Condens. Matter 20 465208

(http://iopscience.iop.org/0953-8984/20/46/465208)

J. Phys.: Condens. Matter **21** (2009) 079801 (1pp) doi:10.1088/0953-8984/21/7/079801

Corrigendum

[1]H-NMR and charge transport in metallic polypyrrole at ultra-low temperatures and high magnetic fields

K Jugeshwar Singh, W G Clark, K P Ramesh and Reghu Menon 2008 *J. Phys.: Condens. Matter* **20** 465208

It has come to the attention of the authors that in the above article a mistake has occured in figure 1. The x-axis label of inset (a) should read T (K), instead of T (mK). Further to this, in the caption of figure 1 it should read $T < 350$ mK instead of $T < 150$ mK.

J. Phys.: Condens. Matter **20** (2008) 465208 (9pp) doi:10.1088/0953-8984/20/46/465208

^{1}H-NMR and charge transport in metallic polypyrrole at ultra-low temperatures and high magnetic fields

K Jugeshwar Singh[1], W G Clark[2], K P Ramesh[1] and Reghu Menon[1]

[1] Department of Physics, Indian Institute of Science, Bangalore 560012, India
[2] Department of Physics and Astronomy, University of California at Los Angeles, 405 Hilgard Avenue, Los Angeles, CA 90095, USA

E-mail: jshwar@physics.iisc.ernet.in

Received 10 July 2008, in final form 17 September 2008
Published 21 October 2008
Online at stacks.iop.org/JPhysCM/20/465208

Abstract

The temperature dependence of conductivity, proton spin relaxation time (T_1) and magnetoconductance (MC) in metallic polypyrrole (PPy) doped with PF_6^- have been carried out at mK temperatures and high magnetic fields. At $T < 1$ K both electron–electron interaction (EEI) and hopping contributes to conductivity. The temperature dependence of a proton T_1 is classified in three regimes: (a) for $T < 6$ K—relaxation mechanism follows a modified Korringa relation due to EEI and disorder, (b) for 6 K $< T <$ 50 K—relaxation mechanism is via spin diffusion to the paramagnetic centers and (c) for $T > 50$ K—relaxation is due to the dipolar interaction modulated by the reorientation of the symmetric PF_6 groups following the Bloembergen, Purcell and Pound (BPP) model. The data analysis shows that the Korringa ratio is enhanced by an order of magnitude. The positive and negative MC at $T < 250$ mK is due to the contributions from weak localization and Coulomb-correlated hopping transport, respectively. The role of EEI is observed to be consistent in conductivity, T_1 and MC data, especially at $T < 1$ K.

1. Introduction

A combined investigation of both conductivity and proton spin lattice relaxation time, especially at very low temperatures and high magnetic fields, is really lacking in metallic conducting polymers. It has been found that the usual studies of conductivity, infrared reflectivity, magnetoresistance, thermopower, etc, are not adequate enough to fully resolve the issues regarding the metallic state in conducting polymers, since it is well known that infinitesimal disorder can localize the states in one-dimensional (1D) electronic systems and it is not trivial to attain the metallic state [1]. Nevertheless, the intrinsic quasi-one-dimensionality and presence of substantial disorder do not hamper the metallic state in many conducting polymers. Although this puzzle has been studied for the past several years, how the delocalized electronic states emerge to form a finite density of states at the Fermi level in such a highly disordered quasi-1D is yet to be understood.

From earlier studies it is known that the metal–insulator (M–I) transition in polypyrrole (PPy) doped with tetrabutylammonium hexafluorophosphate ($TBAPF_6$) can be controlled by varying the extent of disorder [2, 3]. The x-ray diffraction studies have shown that, as crystallinity and crystalline coherence length increases, the system becomes more metallic and the pyrrole rings in ordered regions stack to form quasi-2D type structures [4]. Moreover, high quality samples show a metallic positive temperature coefficient of resistivity (TCR) at $T < 20$ K, with a large finite conductivity (>100 S cm^{-1}) as $T \to 0$ K. Hence PPy–PF_6^- is an ideal system to carry out conductivity and spin–lattice relaxation time studies at mK temperatures [5].

Nuclear magnetic resonance spin lattice relaxation (T_1) is an important experimental parameter to characterize the molecular motions in solids. In metals like Cu, Li, Al, etc, the dominant relaxation mechanism is due to the s-contact hyperfine interaction which couples the nuclear spins

with the conduction electrons and it follows the well-known Korringa relation at low temperatures [6–10]. In contrast, in disordered metals like conducting polymers, etc, in which both electron–electron interaction (EEI) and disorder play dominant roles in low temperature charge transport, the usual Korringa relation is observed to be not satisfactory [11–20]. Such systems tend to have an enhanced Korringa ratio due to the contributions from disorder and EEI [21–23]; hence the simple Korringa relation has to be modified in the case of conducting polymers. In this regard, the temperature dependence of T_1 helps us to understand how the electronic properties are modified in the presence of electron–electron correlation and disorder. The relaxation mechanisms in such systems are mainly due to (1) dipolar interaction between homonuclear spins and heteronuclear spins; (2) interaction of nuclei with conduction electrons (mobile paramagnetic centers) and (3) interaction of the nuclei with the localized, fixed paramagnetic centers [14]. The proton spin relaxation data over a wide range of temperature can sort out the appropriate mechanism.

In this paper the conductivity, *magnetoconductance* (MC) and the proton spin lattice relaxation time in metallic PPy–PF_6^- have been investigated down to 20 mK and at high magnetic fields. T_1 as a function of temperature has been analyzed by using the modified Korringa relation to elucidate the contribution from EEI, disorder, etc, and the different relaxation mechanisms present at various temperature ranges have been analyzed. The role of EEI in low temperature conductivity and MC has been observed, and this is consistent with the enhanced Korringa ratio due to EEI.

2. Experimental details

Highly conducting PPy films, doped with hexafluorophosphate (PF_6^-), are prepared by low temperature electrochemical polymerization at −30 °C [2, 3]. Free-standing films, of thickness ∼20 μm, are peeled off from the electrode for both conductivity and NMR studies. The room temperature conductivity and resistivity ratios [$R_{1.4\ K}/R_{300\ K}$] of samples are ∼300 S cm^{-1} and ∼2, respectively. Magnetoresistance (MR) measurements at very ultra-low temperatures (20 and 70 mK) and high field (0–16 T) were carried out at the National High Field Magnetic Lab at Tellahasse, FL, by the standard four-probe technique, and the current passing through the sample was low enough to avoid any Joule heating effects (less than nanowatts) at mK temperatures [24]. Proton NMR T_1 measurements have been carried out at four different Larmor frequencies (260, 383, 635 and 960 MHz).

3. Result and discussion

3.1. Conductivity studies

The temperature dependence of conductivity of a typical high quality PPy–PF_6 film is shown in figure 1. As reported before, a large finite conductivity (∼150 S cm^{-1}) as $T \rightarrow 0$ K has been observed, indicating the intrinsic metallic nature of these systems. Furthermore, the temperature dependence of conductivity of PPy–PF_6, among various types of conducting

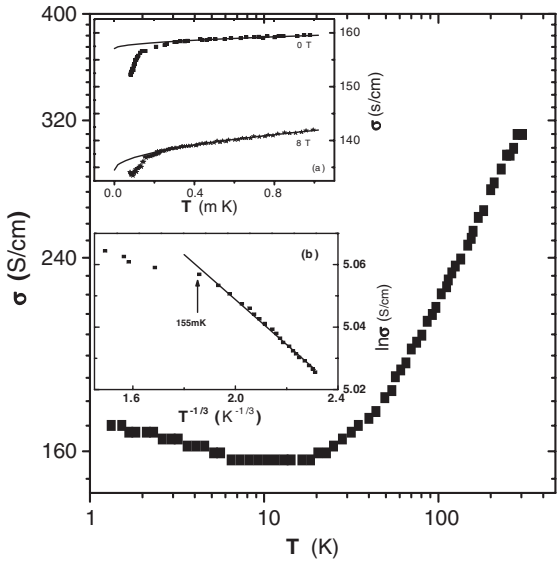

Figure 1. Conductivity versus T for PPy–PF_6. Inset: (a) σ versus T for $T < 1$ K at 0 and 8 T. The solid line is a fit to equation (7). (b) $\ln\sigma$ versus $T^{-1/3}$ for $T < 150$ mK. The solid line is a fit to equation (8).

polymers, is quite peculiar in that a positive temperature coefficient of resistance (TCR) has been observed below 20 K. Even in considerably more metallic conducting polymers like doped oriented polyacetylene this low temperature positive TCR is rarely observed [25]. This, of course, warrants a more detailed investigation of the temperature dependence of conductivity in PPy–PF_6 at millikelvin temperatures. In this regard the earlier studies in PPy–PF_6 were mainly focused at temperatures above 1 K and quantum corrections to low temperature transport have been observed [26]. However, it is of considerable importance to know how this positive TCR and the associated quantum transport evolves at millikelvin temperatures, and this may give more insight into the charge transport mechanism and the nature of the metallic state in such disordered quasi-1D systems at ultra-low temperatures.

The room temperature conductivity of PPy–PF_6 samples is ∼300 S cm^{-1}. These samples show a negative TCR down to 20 K, unlike in the case of metallic polyaniline samples in which a positive TCR was observed down to 150 K [27, 28]. Hence the nature of nanoscale disorder is different, even though the room temperature conductivity of both systems is nearly the same. In the top inset of figure 1, the conductivity data below 1 K, at 0 and 8 T, are shown. Although the conductivity values below 1 K are around 150 S cm^{-1}, the weak negative TCR in the temperature range of 1 K–250 mK indicates the role played by disorder-induced localization, and further below 250 mK the drop in conductivity increases, as shown in the insets in figure 1. Furthermore, the conductivity at 8 T is lower with respect to that at 0 T, suggesting that magnetic field enhances the localization effects, though it is not as severe as that observed in systems near the insulating regime of the metal–insulator transition [26, 28]. Nevertheless, the data for $T < 250$ mK, as shown in inset 'b' of figure 1, fitted to a hopping conduction model, suggest the system is just on the

Table 1. Comparison of the fitted parameters in equation (5*a*) with similar systems.

Sample	Ref.	m (S cm^{-1} K^{-1})	m' (S cm^{-1} K^{-1})	α_1	γF_σ	D (cm^2 s^{-1})
PPy–PF_6 (present work)		2.44	7.35	7.1	0.66	8.1×10^{-2}
PEDOT–PF_6[a]	[32]	−3.02	7.03	7.66	1.56	6.9×10^{-2}
PANI–AMPSA	[27]	—	—	9.59	—	4.4×10^{-2}
PANI–CSA	[33]	10.8	19.8	18.3	0.5	1.25×10^{-2}

[a] PEDOT–PF_6: poly(3,4-ethylenedioxy-thiophene)–PF_6.

insulating side at ultra-low temperatures, in spite of the large finite conductivity. This indicates that disorder affects the inter-chain transport and metallic state at ultra-low temperatures.

This data in inset 'a' of figure 1 has been analyzed by using the interaction–localization model for a disordered metallic system, and the fit looks satisfactory in the low temperature region, till the data deviates below 250 mK. According to this model the conductivity can be expressed as [29–31]

$$\sigma(T) = \sigma(0) + mT^{1/2} + BT^{p/2} \tag{1}$$

$$m = \alpha_1 \left[\tfrac{4}{3} - \tfrac{3}{2}\gamma F_\sigma\right] \tag{2}$$

$$\alpha_1 = \left[\frac{e^2}{\hbar}\right]\left[\frac{1.3}{4\pi^2}\right]\left[\frac{k_B}{2\hbar D}\right]^{1/2} \tag{3}$$

where $\sigma(0) \sim 0.1e^2/\hbar L_{corr}$ (L_{corr} being the correlation length) and γF_σ is the interaction term ($\gamma F_\sigma > 0$). Here the value of γ depends on the band structure, F_σ is the Hartree factor and α_1 in equation (3) is expressed in terms of D, where D is the diffusion coefficient. The second term in equation (1) is the lowest order correction to the conductivity arising from electron–electron interactions (EEI) and the third term is the finite temperature localization correction to the less disordered limit. The third term is determined by the temperature dependence of the inelastic scattering rate $\tau_{in}^{-1}(\propto T^p)$ of the dominant dephasing mechanism. For electron–phonon scattering, $p = 2.5$–3; for inelastic electron scattering, $p = 2$ and 1.5 in the clean and dirty limits, respectively. Both $\sigma(0)$ and the pre-factor m depend on the magnetic field as well as on pressure [25, 26]. In disordered metals, EEI plays an important role in low temperature transport and the third term is not considered for the analysis. The EEI contribution to the low temperature conductivity at zero magnetic field $\sigma_I(T)$ can be expressed as

$$\sigma(T) \to \sigma_I(T) = \sigma(0) + mT^{1/2}. \tag{4}$$

However, in the presence of sufficiently high fields such that $g\mu_B H \gg k_B T$, where g is the g value of an electron and μ_B is the Bohr magneton (i.e. when the field exceeds the limit of Zeeman splitting), equation (4) gets modified to equation (5):

$$\sigma_I(H, T) = \sigma(H, 0) + m'T^{1/2} \tag{5a}$$

$$m' = \alpha_1 \left[\tfrac{4}{3} - \tfrac{1}{2}\gamma F_\sigma\right] \tag{5b}$$

where $\sigma(0)$ and m in equation (4) change to $\sigma(H, 0)$ and m' in equation (5*a*). The data in the inset in figure 1 at 0 and 8 T are fitted to equations (4) and (5*a*), respectively. The fitted parameters are $m = 2.44$ S cm^{-1} K$^{-1/2}$ and $m' = 7.35$ S cm^{-1} K$^{-1/2}$. This gives $\alpha_1 \sim 7.1$ S cm^{-1} K$^{-1/2}$ and $\gamma F_\sigma \sim 0.66$, which in turn gives the diffusion constant, $D = 8.1 \times 10^{-2}$ cm^2 s^{-1}. A comparison of these parameters with those reported in similar systems has been compiled in table 1. The values of α_1 and γF_σ are in close agreement with the earlier reports [27, 32, 33]. However, the data below 250 mK deviate from this model, as in inset 'a' of figure 1. As mentioned before this decrease in conductivity is due to the disorder-induced hopping transport at ultra-low temperatures. The best fit to the conductivity below 155 mK follows a $T^{-1/3}$ dependence, which can be ascribed to the dominant role of hopping transport among the slightly disordered 2D regions in the system. Furthermore, the implications of this variation in charge transport above and below 250 mK are observed in magnetoconductance data, as described in section 3.3.

3.2. Proton spin lattice relaxation (T_1)

Proton T_1 experiments have been carried out at 260, 383, 635 and 960 MHz as a function of temperature. The measurements at ultra-low temperature from 50 mK to 10 K are carried out at 260 and 635 MHz, while in the range of 1–300 K at 383 and 960 MHz. The proton $(1/T_1)$ versus temperature plot at all four frequencies is shown in figure 2, and T_1 is observed to be dependent on both frequency and temperature. Part of these studies was reported by Clark *et al* [34]. We have also given a plot of $1/T_1$ versus T of copper in figure 2 for comparison. In a conventional metal, $1/T_1 \propto T$ (Korringa relaxation) and is independent of the field (B_0) or NMR frequency (f_{NMR}) except for extremely low T. However, when there is thermal expansion of the lattice, a small variation from $1/T_1 \propto T$ occurs. The reason $1/T_1$ is independent of B_0 in a conventional metal is that the correlation time for the fluctuation of the hyperfine field from conduction electrons is very short ($\sim 10^{-15}$ s, the time for the conduction electron to cross a hydrogen atom $\approx$ (atomic separation/Fermi velocity)) and has a very small variation throughout the sample. This condition generates a power spectrum $J(\omega)$ that is independent of f_{NMR} throughout the NMR frequency range and leads to a $1/T_1$ that is independent of B_0, or f_{NMR}.

Earlier T_1 relaxation studies, at lower frequencies, in metallic polyacetylene and polyaniline have shown weaker temperature dependences [12]. In a conducting polymer, like the present one, which have hopping conductivity at lower temperatures, regions with different electron motion dynamics, significant electron–electron interactions, etc, it is expected that there will be a broad distribution of correlation times (τ_c)

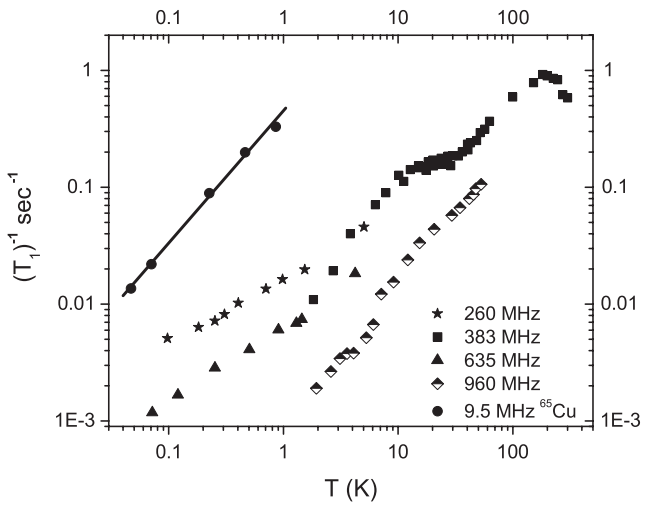

Figure 2. ^{1}H-NMR T_1 versus T for PPy–PF_6. The $1/T_1$ versus T of ^{65}Cu at 9.5 MHz (●) [7] is shown. The solid line is a guide to the eye.

for the hyperfine field at the proton sites that will make $J(\omega)$ to have a significant variation as a function of ω, which in turn will make the proton $1/T_1$ dependent on B_0 (or f_{NMR}). If this distribution of τ_c has significant values for $\tau_c > 1/\omega_{\mathrm{NMR}}$, it will cause a contribution to $1/T_1$ that decreases with increasing f_{NMR}, which is observed in our measurements.

The analysis of T_1 is carried out in different ranges of temperatures. In metallic PPy–PF_6, the possible relaxation mechanisms are mainly due to Korringa type, especially at low temperatures; and at higher temperatures due to fluctuation of the local fields resulting from the interaction between the magnetic moments of protons, fluorine nuclei and the paramagnetic centers. Each of these mechanisms will contribute to the relaxation process depending on the temperature range under consideration.

The main relaxation mechanism for the increase in T_1 as a function of frequency is explained by considering the dipolar coupling between nuclear spins and conduction electrons. In this case T_1 is proportional to the square of the applied magnetic field H_0 (i.e. working frequency) [35]. This is supported by the observed values of T_1 values at two magnetic fields of 22 and 9 T, as in figure 2. Nevertheless, in typical metals like Cu this frequency dependence of T_1 is not usually observed. This indicates that the frequency dependence of T_1 in PPy–PF_6 is due to the contributions from disorder that play a role in the relaxation mechanisms. However, this aspect requires more detailed investigations. Also it is interesting to compare how much T_1 varies as a function of temperature in various systems. In usual metals like Cu the variation of T_1 as a function of temperature (1–300 K) is limited to three orders of magnitude [7], while in organic conductors like fluoranthenyl–PF_6 it changes by one order [14]. However, T_1 in disordered systems like metallic glasses (for example, TiCuHx) changes by one order of magnitude, in the temperature range 111–500 K [36]. In metallic PPy–PF_6, T_1 is observed to vary by two orders of magnitude; hence this behavior is intermediate between that of conventional metals and disordered metallic glasses.

3.2.1. T_1 data analysis for temperature below 6 K. The large finite conductivity at ultra-low temperatures show the intrinsic metallic nature of the system, though a slight nonmetallic behavior arises due to disorder at $T < 250$ mK. Hence it will be quite interesting to verify how far the usual models to analyze the proton T_1 versus temperature data for disordered metallic systems are applicable in the case of PPy–PF_6. In order to simplify this procedure it is better to understand the T_1 behavior starting with a well-known model system, for example, the non-interacting electrons in alkali metals. In alkali metals, the s-contact interaction represents the only hyperfine coupling mechanism between non-interacting conduction electrons and nuclear spins (with a gyromagnetic ratio γ_n). Then the nuclear spin lattice relaxation time T_1 is related to the Knight shift K via the well-known Korringa relation [6, 37]:

$$K^2 T_1 T = \left(\frac{\gamma_e}{\gamma_n}\right)^2 \left(\frac{\hbar}{4\pi k_B}\right) \tag{6}$$

where γ_e is the electronic gyromagnetic ratio, and k_B and $\hbar$ are the Boltzmann constant and the reduced Planck's constant, respectively. It is known that spin–lattice relaxation is a stronger indicator of the hyperfine interaction of nuclei with free charge carriers than the Knight shift; and due to this the spin–lattice relaxation rate is observed to be inversely proportional to T in the usual metals, as shown by Korringa [6].

Nevertheless equation (6) cannot be directly used to explain the T_1 versus T behavior since conducting polymers are morphologically very different from the usual metals. Obviously, electron correlations and Coulombic repulsions are not dealt with in the derivation of the Korringa relation for metals, and these may be significant in conducting polymers. In this context Narath and Weaver pointed out that, in the presence of EEI, the Knight shift in alkali metals is enhanced by the Stoner factor contribution to that of the free charge carrier [21, 22]. In addition to this, Shastry and Abrahams have shown that the relaxation rate (and thus the Korringa ratio) is significantly enhanced by disorder [23]. Thus, the Korringa relation for normal metals has to be modified by taking into consideration the contributions due to EEI and disorder, and especially in the context of organic and polymeric conductors. The first theoretical approach to modify the Korringa relation was attempted by Soda *et al* in organic conductor systems [11]. This was later expanded by Mehring and coworkers for A_3C_{60} (where A = AsF_6^-, SbF_6^-, PF_6^-) systems, as [12, 13, 38]

$$K^2 T_1 T \left(1 + \frac{\varepsilon}{2}\right) C_o S_K = 1 \tag{7}$$

where $C_0 = (\gamma_n/\gamma_e)^2(4\pi k_B/\hbar)$, ε (= Knight shift anisotropy = d^2/a^2) is the ratio of the anisotropic and isotropic contributions to the hyperfine interaction [12], which plays an important role in the relaxation of organic materials, and S_K is the Korringa enhancement factor which has taken EEI into consideration along with disorder contributions. The Korringa enhancement factor contains the spectral density of interaction [13] and is expressed as

$$S_K = \frac{1}{2}\left(\frac{\tau_\perp}{\tau_s}\right)^{1/2}\left[\frac{3}{5}\varepsilon J(\omega_n) + \left(1 + \frac{7}{5}\varepsilon\right) J(\omega_e)\right] K_0(\alpha) + \tfrac{1}{2}(1 + 2\varepsilon)\, K_{2k_F}(\alpha). \tag{7a}$$

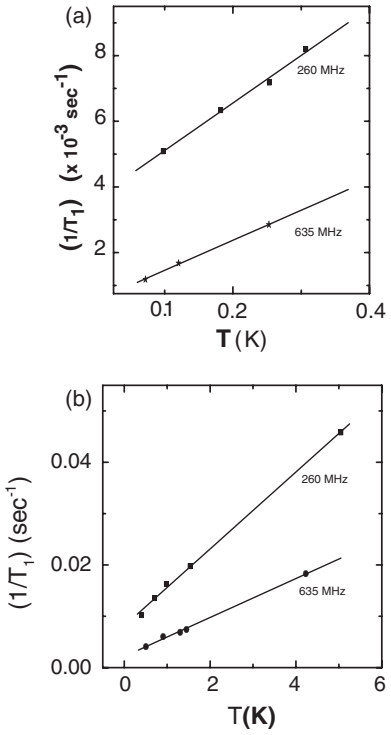

Figure 3. (a) ^{1}H-NMR T_1 versus T for $T < 400$ mK. Straight lines are fits to equation (7) and the parameters are shown in table 2. (b) ^{1}H-NMR T_1 versus T for 400 mK $< T <$ 6 K. Straight lines are fits to equation (7) and the parameters are shown in table 2.

In this expression $\tau_\perp$ is the inter-chain hopping time, τ_s is the phonon scattering time along the chain and α is the Coulombic repulsion energy. The quantity $\varepsilon(= d^2/a^2)$ is the ratio of anisotropic to isotropic contribution of the hyperfine interaction and $J(\omega)$ $\{= [(1+\omega^2\tau_\perp^2)^{1/2}+1]/[2(1+\omega^2\tau_\perp^2)]\}$, is the spectral density of interaction with ω_e and ω_n being the electron and nuclear precession frequencies, respectively. In addition to this, $K_0(\alpha)$ and $K_{2k_F}(\alpha)$ are given by the expressions: $K_0(\alpha) = (1-\alpha)^{1/2}$ and $K_{2k_F}(\alpha) = (1-\alpha)^2/[1-\alpha F(2k_F)]^2$; $F(2k_F) = (1/2)[\ln(4.56T_F/T)]$, the Lindhart function and T_F is the Fermi temperature. For classical metals, $\varepsilon = 0$ and $S_K = 1$, and the Korringa relation is recovered. In organic conductors, for example fluoranthene–PF_6, with highly anisotropic conduction, S_K has values from 50 to 500 and $0 < \varepsilon < 4$, showing a large deviation from that of a classical metal [39].

The fits for ^{1}H–T_1 data at 260 and 635 MHz in the temperature range 50–350 mK (figure 3(a)) and 350 mK to 5 K (figure 3(b)) to equation (7) yield straight lines with different slopes, and they do not pass through the origin. The straight line fit corresponds to the Korringa-type relaxation in this temperature range. The change in slopes is related to the change in Knight shift, and the parameters obtained by fitting the data to equation (7) are compiled in table 2. The observed enhancement in Knight shift is due to: (i) EEI and (ii) the disorder effect. At these ultra-low temperatures, the relaxation due to paramagnetic centers can be ruled out as these gets saturated around 4 K for 260 MHz and 10 K for 635 MHz. Also, other interactions, such as reorientation and heteronuclear interaction, are ruled out at millikelvin temperatures. An important feature of these fits is that they show a positive intercept, which implies a finite relaxation time even at $T = 0$ K, and this is attributed to the EEI contribution to the relaxation mechanism.

Table 2. Parameters of proton spin lattice relaxations (^{1}H-SLR) in PPy–PF_6 derived from the fit to equation (7) (at $\kappa = 10$ ppm and $\epsilon = 2$).

Temperature (T)	S_K (at 260 MHz)	S_K (at 635 MHz)
20 mK $< T <$ 350 mK	19	12
350 mK $< T <$ 5 K	9.8	5

The above analysis show the importance of EEI and disorder in the Korringa ratio, $\kappa = C/(K^2T_1T)$, where $C = (\gamma_e/\gamma_n)^2(\hbar/4\pi k_B)$. The model developed by Shastry and Abrahams [23] shows how the Korringa ratio varies as a function of EEI and disorder. For example, as interaction strength increases from 0 to 1 the Korringa ratio varies from 0.2 to 2.7, and this variation is related to the total Korringa enhancement (S), which according to this model varies from 10 to 60. Also, these variations increase when the order parameter for disorder ($k_F\lambda$, where k_F is the Fermi wavevector and λ is the mean free path) decreases [23]. Typically in organic conductors, the Knight shift is in the range of 10–15 ppm and taking $\varepsilon \sim 2$ (since $0 < \varepsilon < 4$) gives the Korringa enhancement factor, S_K of 5–19, which in turn yields the enhanced Korringa ratio in PPy–PF_6 by a factor of 10–40. Hence, knowing the value of S (10–40) and $k_F\lambda$ (∼1.2), the interaction strength can be determined and is found to vary from 0.45 to 0.8. Furthermore, this enhancement in Korringa ratio is also related to the ratio of magnetic susceptibility ($\kappa = S(\chi_0\chi^{-1})^2$, where χ_0 is the dynamical susceptibility incorporating the effects of disorder but not due to interaction and χ is the Pauli spin susceptibility). Thus, from the already known values of κ and S, the ratio of $(\chi_0\chi^{-1})$ can be determined and it is estimated to be in the range of 0.44–0.22. Hence the χ_0 is less than χ by a factor of 2.27–4.5, implying that the enhancement in κ is more due to interaction than from disorder (i.e. localization effects). The consistency of this analysis is further verified by comparing the values of interaction parameter obtained from this analysis to that from the low temperature conductivity data. From equations (5*a*) and (5*b*), the interaction parameter (γF_σ) is found to be ∼0.66 (the analysis of MC data gives 0.8, as shown in section 3.3). Hence the range of values for the interaction parameter obtained from this modified Korringa analysis (0.45–0.8) is quite consistent with that obtained from the conductivity and MC data analysis.

The S_K values obtained in the temperature range of 50–350 mK is almost twice than that obtained in the temperature range of 350 mK–5 K. The first and second terms in equation (7*a*) can be neglected as there is no possibility of phonon scattering at these mK temperatures, hence only the third term is considered for data analysis. Therefore S_K mainly depends on the hyperfine anisotropy, ε and the Coulombic repulsion energy α. Since ε is nearly constant, the change in S_K is mainly due to α, i.e. the electron–electron interaction. From

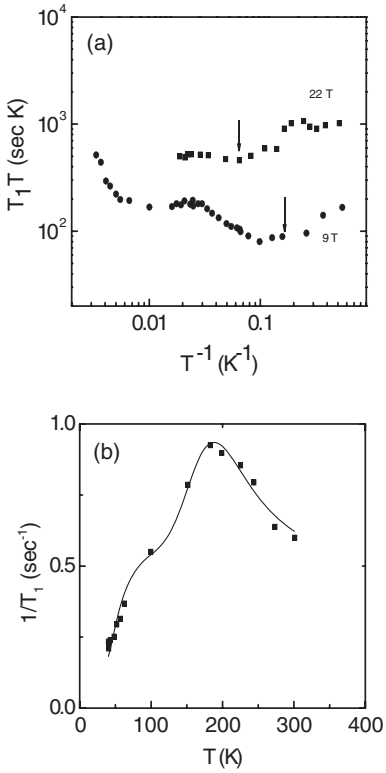

Figure 4. (a) ^{1}H-NMR (T_1T) versus T^{-1}. Arrows are shown for the values of T at $g\mu_B = 2k_BT$. (b) ^{1}H-NMR T_1 versus T at Larmor frequency 383 MHz. The solid line is a fit to equation (8) and the parameters are shown in table 3.

equation (7*a*) it is clear that the higher value of S_K is attributed to higher values of α, implying strong EEI contributions to the relaxation mechanism at mK temperatures, which is consistent with both conductivity and magnetoresistance (as explained in section 3.3) data.

3.2.2. T_1 analysis from 6 to 50 K. The following relaxation mechanisms are taken into account for the analysis of ^{1}H–T_1 data (at 383 MHz) in the temperature range of 6–300 K: (i) via spin diffusion to paramagnetic centers, (ii) the translational and orientational motion of electronic spins and (iii) reorientational motion of symmetric subgroups in the polymer chain. In some particular temperature range the motion of electron spins via spin diffusion to paramagnetic centers (SDPC) is the dominant contribution to proton spin lattice relaxation. However, this mechanism freezes out at high magnetic fields and low temperatures. At these conditions the Zeeman energy is enough to saturate the magnetization of isolated and pinned electrons, and no longer contributes to the relaxation mechanism via SDPC. This is evidently seen from the temperature-independent T_1T, in figure 4(a), for 6–50 K. The vertical arrows (in figure 4(a)) indicate where the Zeeman energy $g\mu_BB = 2k_BT$, below which the SDPC process is expected to freeze out (g is the electron g factor, μ_B is the Bohr magneton and $2k_B$ is the Boltzmann constant [34]). Accordingly proton relaxation via SDPC should freeze out at around 6 K for 383 MHz and 15 K for 960 MHz. Although the observed behavior indicates that this mechanism contributes up to about 50% of the total rate, however, the proton relaxation due to the translational motion of electrons, especially at low temperatures, is expected to make some contribution too. As the dc conductivity (see figure 1) is relatively large, and its temperature dependence is rather weak in the range from 6 to 30 K, the proton spin–lattice relaxation due to the dipolar interaction between conduction electrons and protons can be equally dominant as the contribution from the SDPC in this temperature range. The increase in T_1T at higher temperatures is attributed to the relaxation due to the reorientation of PF_6 groups which follow the BPP model [40], as described below.

Table 3. Parameters of proton spin–lattice relaxations (^{1}H-SLR) in PPy–PF_6 derived from the fit to equation (8). For definitions of the parameters, see [21, 22] and the text.

K_{HH} (s^{-2})	K_{HF} (s^{-2})	$\tau_{\infty,HH}$ (s)	$\tau_{\infty,HF}$ (s)	ΔE_{HH} (meV)	ΔE_{HF} (meV)
2.7×10^{10}	14.92×10^{7}	2.07×10^{-12}	27.06×10^{-10}	79.02	0.91

3.2.3. T_1 analysis above 50 K. The T_1 behavior at temperatures above 50 K, at 383 MHz, is interpreted in terms of the reorientational motion of symmetric groups such as PF_6. The relaxation of protons is due to the ^{19}F–^{1}H magnetic dipolar interactions that are modulated by PF_6 reorientation jumps, hydrogen–hydrogen interaction, pyrrole librational and vibrational motions. The corresponding rate equation in the BPP model can be expressed as [14–16, 41, 42]

$$(T_1)^{-1}_{BPP} = K_{HF}[J(\tau_{HF}, (\omega_H - \omega_F)) + 3J(\tau_{HF}, \omega_H) + 6J(\tau_{HF}, (\omega_H + \omega_F))] + K_{HH}[J(\tau_{HH}, \omega_H) + 4J(\tau_{HH}, 2\omega_H)] \quad (8)$$

where $J(\tau_i, \omega_N) = \frac{\tau_i}{1+(\omega_N\tau_i)^2}$ and a simple Arrhenius law for τ_i: $\tau_i = \tau_{\infty i}e^{\frac{\Delta E_i}{k_BT}}$.

The proton relaxation rate exhibits a maximum around 180 K, as shown in figure 4(b). This type of behavior is usually seen in systems in which the reorientational motion plays a dominant role in the relaxation mechanism, and this is attributed to the BPP model (as in equation (8)). The fitted parameters are compiled in table 4. The values of K_{HF} and K_{HH} [35, 42] (see table 3) are obtained by fitting the experimental values of T_1 to equation (8). The value of K_{HF} is pertinent to the proton relaxation process via the fluorine atoms in PF_6 counter-ions situated in between the PPy chains, and this is related to the inter-chain charge transport. It is known that this type of molecular motion can influence the relaxation rate at high temperatures. Similar behavior has been observed in organic conductors like fluoranthenyl–PF_6 [14] and in pyrene–hexafluoroantimonate [16]. Since the interaction constants are inversely proportional to r^6 (where r is the internuclear distance), the contribution to the values of T_1 is substantially weaker from nuclei situated in the 100 (∼7.3 Å) and 010 (∼6.7 Å) lattice directions in the PPy–PF_6 structure. However, the contribution to T_1 from the nuclei in the interplanar direction of 001 (∼3.5 Å) is quite significant.

Table 4. Transport parameters from the magnetoconductance fit to equation (10).

Temperature	$\eta(T)$	A_e	B_i ($\times 10^{-2}T$)	$B_e(T)$	τ_i ($\times 10^{-14}$ s)
20 mK	0.275	1.13	7.23	11.598	2.32
70 mK	0.312	1.30	7.5	8.849	2.23

The K_{HF} values from the fit can give an estimate for the value of r (i.e. the H–F vector) = 3.8 Å. This value, obtained from the fit to equation (8), is quite close to the value of 3.5 Å for the interplanar distance, as observed from the x-ray data for PPy–PF_6 films [4, 5]. This finding suggests that the analysis of NMR data using equation (8) is quite appropriate.

3.3. Magnetoconductance analysis

The above data analysis shows the importance of electron–electron correction effects in both low temperature conductivity and proton spin relaxation time. It is well known that EEI can play a significant role in low temperature MC in disordered metallic systems, and the previous MC studies at $T > 1$ K in PPy–PF_6 have indicated the same; however, the MC data for $T < 1$ K have shown some anomalous features.

The MC data for metallic PPy–PF_6 at 500, 370, 70 and 20 mK are shown in figure 5. The data show contributions from both positive and negative MC, whereas the MC for $T > 1$ K is negative at all fields. Hence for $T < 1$ K an additional mechanism is contributing to the MC. At 500 and 370 mK, the MC is slightly negative at low fields and it becomes positive at higher fields. This type of behavior is expected when both weak localization (i.e. positive MC) and EEI (i.e. negative MC) are contributing to the MC. At high fields, the MC arises mainly from the interaction contribution, since the weak localization contribution is less important at strong fields, especially at $T > 300$ mK [30]. The EEI contribution to high field MC is given by

$$\Delta\Sigma_I(H,T) = \sigma(H,T) - \sigma(0,T)$$
$$\Delta\sum_I(H,T) = \alpha_1\gamma F_\sigma T^{1/2} - 0.77\alpha_1(g\mu_B/k_B)^{1/2}\gamma F_\sigma H^{1/2}$$
$$g\mu_B H \gg k_B T. \tag{9}$$

The straight line fit, for the data at 500 and 370 mK, to equation (9) is shown in the inset of figure 5. From the slope of the $H^{1/2}$ fits, the value of γF_σ can be determined as 0.80, which is rather close to the value of $\gamma F_\sigma (= 0.66)$ obtained from conductivity data from equations (2) and (5*b*). This validates the internal consistency in the data analysis. Moreover this value of γF_σ is quite similar to the values reported in earlier work [2]. This confirms the role of EEI in low temperature conductivity, proton spin relaxation and MC.

The MC data for 20 and 70 mK are quite different from those observed at higher temperatures, as shown in figure 5. The positive MC is unusually large (>40%) and it decreases considerably at higher magnetic fields. This is expected since the temperature dependence of conductivity below 155 mK is dominated by hopping transport, as shown in the inset of figure 1. However, this large positive MC cannot be accounted

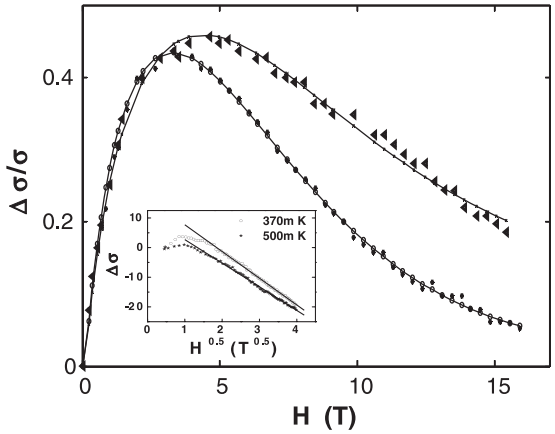

Figure 5. $\Delta\sigma/\sigma$ versus **H** for PPy–PF_6 at 70 mK (Δ) and 20 mK (○). The solid line is a fit to equation (10) and the parameters are shown in table 4. Inset: $\Delta\sigma$ versus $\mathbf{H}^{0.5}$ for PPy–PF_6 at 370 mK (○) and 500 mK (∗). The solid line is a fit to the linear equation (9).

for within the conventional weak localization and EEI model, since the upper limits of quantum corrections to MC are less than 10%. Nevertheless, in some systems large positive MC has been observed due to various other types of mechanism. For example, in pregraphitic carbon nanofibers [43, 44], non-magnetic granular materials [45] and granular aluminum at the boundary of the superconducting transition [46], such large positive MC has been reported. Also in systems near the M–I transition, the mobility edge can be shifted by an external magnetic field, especially when the magnetic length $L_H (= \hbar c/eH)^{1/2}$ becomes comparable to the localization length (L_c), and a shift in the mobility edge (E_c) is proportional to $(L_H/L_c)^{1/\eta}$, where h is Planck's constant and c is the velocity of light [45–47]. Furthermore, Wang *et al* have pointed out another possibility, that the magnetic field can shift the energy levels of carriers via the Zeeman effect, and this can enhance the phonon-assisted hopping and a large decrease in resistance; however, this mechanism is expected at $T > 1$ K [43–45]. However, these mechanisms cannot comprehensively explain both the positive and negative contributions to MC observed in PPy–PF_6, at $T < 300$ mK.

The MC data at $T < 300$ mK clearly show the presence of two mechanisms that give rise to the large positive MC at lower fields, and then its decrease at higher fields. In PPy–PF_6, x-ray diffraction data show the presence of 2D regions in the system, and the positive MC can account for the charge transport and scattering mechanism within these 2D regions. Hikami *et al* have shown that in weakly disordered 2D systems with negligible spin–orbit coupling and magnetic scattering, the positive MC can be large at low fields, and this contribution is expressed by the first part on the right-hand side of equation (10) [48]. This mechanism is the dominant contribution to the positive MC, although the observed values of MC are larger due to the specific nanoscopic scale structural features of this system in studies [4, 5]. Also possibly some of the above-mentioned mechanisms for positive MC might contribute too, yet the fit to equation (10) is observed to be quite satisfactory. However, at fields above 4 T, the positive

MC starts to decrease, as observed at both 70 and 20 mK. This clearly shows the role of another mechanism, especially at higher fields. Kurobe and Kamimura have suggested a model based on the field-induced interaction among singly, doubly and unoccupied states in a disordered system with on-site Coulomb repulsion [49]. This contribution is largely arising from the scattering process involved in some of the highly disordered 2D regions in the system that also give rise to the observed $T^{-1/3}$ dependence of conductivity at ultra-low temperatures. Hence a combination of these two mechanisms, as expressed in equation (10), can fit the data in the entire range of magnetic fields [28, 38]. This type of behavior in MC has been observed by Wang *et al* [43] in carbon nanofibres and by Song *et al* [44] in nanotubes:

$$\frac{\Delta\sigma}{\sigma(0,T)} = -\eta(T)\left[\Psi\left(\frac{1}{2}+\frac{B_i}{H}\right) - \log\left(\frac{B_i}{H}\right)\right] + A_e\frac{H^2}{H^2+B_e^2} \tag{10}$$

where ψ is the digamma function, H is the magnetic field, $B_i = h/(4eD\tau_i)$ is the inelastic scattering equivalent magnetic field, D is the diffusion coefficient, τ_i is the inelastic scattering time, A_e is a constant (the saturation of the MC) that indicates the EEI contribution to MC and B_e is the characteristic field for spin alignment. The first and second parts on the right-hand side of equation (10) represent the contributions arising from 2D weak localization (in ordered 2D regions) and Coulomb correlation in hopping transport (in disordered 2D regions), respectively [50]. The fitted parameters are shown in table 4. From these parameters the values for τ_i can be evaluated, at 70 and 20 mK, by using the equation $\tau_i = h/(4eDB_i)$. The calculated values of τ_i are in agreement with the reported values [51]. Thus, the analysis of MC data, at ultra-low temperatures, by using equation (10) is quite appropriate. Since the values of A_e are quite large the Coulomb correlation effects are expected to be significant, as is also found from the earlier analysis of NMR data. Hence the analysis of both NMR and MC data is observed to be consistent regarding the importance of Coulomb correlation effects at very low temperatures.

4. Conclusions

The conductivity, proton spin relaxation time (T_1) and magnetoconductance (MC) in metallic PPy–PF_6, at mK temperatures and high magnetic fields, show the significance of both EEI and disorder in the charge transport properties of conducting polymers.

The mechanisms for T_1 relaxation, at various temperature ranges, are as follows:

(a) the proton T_1 versus temperature data follow a linear fit, in the temperature range from 50 to 300 mK, as expected from the Korringa relation; however, the positive intercept, as well as the enhancement in Korringa ratio, imply that the relaxation mechanism is dominated by the EEI contribution at ultra-low temperatures.

(b) in the intermediate temperature range of 1–40 K, the SDPC and translational motion of conduction electrons are responsible for the proton spin–lattice relaxation. Proton spin–lattice relaxation is due to the SDPC for $T \sim$ 6–40 K; and this contribution freezes out at $T \sim 15$ K for 22.6 T and at $T \sim 6$ K for 9 T, when the magnetization of paramagnetic centers saturates.

(c) in the high temperature range of 50–300 K, the dipolar interaction of ^{1}H–^{1}H and ^{1}H–^{19}F modulated by the reorientational motion of symmetric groups such as PF_6, and librational, vibrational motion of polymer chain are responsible for the relaxation.

The MC data show two different behaviors. At $T >$ 250 mK, the negative MC follows an $H^{1/2}$ dependence, indicative of the dominance of the EEI contribution. However, at $T <$ 100 mK both positive and negative MC are observed, and this is mainly due to the dominant contributions from weak localization and Coulomb correlations in hopping transport, respectively; and the fit shows the latter is more significant.

Acknowledgment

The authors would like to thank DST and NSF for funding; especially to M Horvatic, C Berthier, Guo-qing Zheng, P Kuhns and W G Moulton for their help in experiments.

References

[1] Reghu M 1997 *Handbook of Organic Conductive Molecules and Polymers* vol 4, ed H S Nalwa (New York: Wiley) p 47
[2] Yoon C O, Reghu M, Moses D and Heeger A J 1994 *Phys. Rev.* B **49** 10851
[3] Hagiwara T, Hirasaka M, Sato K and Yamaura M 1990 *Synth. Met.* **36** 241
[4] Nogami Y, Pouget J P and Ishiguro T 1994 *Synth. Met.* **62** 257
[5] Yoon C O, Sung H K, Kim J H, Barsoukov E, Kim J H and Lee H 1999 *Synth. Met.* **99** 201
[6] Korringa J 1950 *Physica* **16** 601
[7] Bloembergen N 1949 *Physica* **15** 588
[8] Hatton J and Rollin B V 1949 *Proc. R. Soc.* A **199** 222
[9] Norberg R E and Slichter C P 1951 *Phys. Rev.* **83** 1074
[10] Poulis N J 1950 *Physica* **16** 373
[11] Soda G, Jerome D, Weger M, Alizon J, Gallice J, Robert H, Fabre J M and Giral L 1977 *J. Physique* **38** 931
[12] Kolbert A C, Caldarelli S, Thier K F, Sariciftci N S, Cao Y and Heeger A J 1995 *Phys. Rev.* B **51** 1541
[13] Thier K F, Goze C, Mehring M, Rachdi F, Yildrim T and Fischer J E 1999 *Phys. Rev.* B **59** 10536
[14] Hoptner W, Mehring M, Von Schutz J U, Wolf H C, Morra B S, Enkelmann V and Wegner G 1982 *Chem. Phys.* **73** 253
[15] Sachs G and Dormann E 1988 *Synth. Met.* **25** 157
[16] Kaiser A, Pongs B, Fischer G and Dormann E 2001 *Phys. Lett.* A **282** 125
[17] Paalanen M A, Ruckenstein A E and Thomas G A 1985 *Phys. Rev. Lett.* **54** 1295
[18] Alloul H and Dellouve P 1987 *Phys. Rev. Lett.* **59** 578
[19] Mizoguchi K 1995 *Japan. J. Appl. Phys.* **34** 1
[20] Lee H O and Choi H Y 2000 *Phys. Rev.* B **62** 15120
[21] Narath A and Weaver H T 1968 *Phys. Rev.* **175** 373
[22] Robert W S Jr and Warren W W Jr 1971 *Phys. Rev.* B **3** 1562
[23] Shastry B S and Abrahams E 1994 *Phys. Rev. Lett.* **72** 1933
[24] Clark J C, Ihas G G, Rafanello A J, Meisel M W, Reghu M, Yoon C O, Cao Y and Heeger A J 1995 *Synth. Met.* **69** 215

[25] Menon R, Väkiparta K, Cao Y and Moses D 1994 *Phys. Rev.* B **49** 16162
[26] Menon R, Yoon C O, Moses D and Heeger A J 1994 *Synth. Met.* **64** 53
[27] Mukherjee A K and Reghu M 2005 *J. Phys.: Condens. Matter* **17** 1947
[28] Menon R, Väkiparta K, Yoon C O, Moses D and Heeger A J 1994 *Synth. Met.* **65** 167
[29] Lee P A and Ramakrishnan T V 1985 *Rev. Mod. Phys.* **57** 287
[30] Peihua D, Youzhu Z and Sarachik M P 1992 *Phys. Rev.* B **46** 6724
[31] Altshuler B L and Aronov A G 1979 *JETP Lett.* **30** 968
[32] Aleshin A, Kiebooms R, Reghu M, Wudl F and Heeger A J 1997 *Phys. Rev.* B **56** 3659
[33] Reghu M, Yoon C O, Moses D and Heeger A J 1993 *Phys. Rev.* B **48** 17685
[34] Clark W G, Tanaka K, Brown S E, Menon R, Wudl F, Moulton W G and Kuhns P 1999 *Synth. Met.* **101** 343
[35] Abragam A 1991 *The Principles of Nuclear Magnetism* (Oxford: Oxford University Press) p 380
[36] Robert C B Jr and Arnulf J M 1981 *Phys. Rev.* B **24** 2328
[37] Slichter C P 1989 *Principles of Magnetic Resonance* 3rd edn (Heidelberg: Springer) p 156
[38] Mehring M 1987 *Low Dimensional Conductors and Superconductors* ed D Jerome and L S Caron (New York: Plenum) p 185
[39] Köngeter D and Mehring M 1989 *Phys. Rev.* B **39** 6361
[40] Bloembergen N, Purcell E M and Pound R V 1948 *Phys. Rev.* **73** 679
[41] Nemec G, Illich V and Dorman E 1998 *Synth. Met.* **95** 149
[42] Tso C H, Madden J D and Michal C A 2007 *Synth. Met.* **157** 460
[43] Wang Y and Santiago-Avilés J J 2006 *Appl. Phys. Lett.* **89** 12119
[44] Song S N, Wang X K, Chang R P H and Ketterson J B 1994 *Phys. Rev. Lett.* **72** 697
[45] Wang X R, Ma S C and Xie X C 1999 *Europhys. Lett.* **45** 368
[46] Sin H K, Lindenfeld P and McLean W L 1984 *Phys. Rev.* B **30** 4067
[47] Shlvoskii B I and Efros A L 1984 *Electronics Properties of Doped Semiconductors* (Heidelberg: Springer)
[48] Hikami S, Larkin A I and Nagaoka Y 1980 *Prog. Theor. Phys.* **63** 707
[49] Kurobe A and Kamimura H 1982 *J. Phys. Soc. Japan* **51** 1904
[50] Frydman A and Ovadyahu Z 1995 *Solid State Commun.* **94** 75
[51] Lee K, Miller E K, Aleshin A N, Reghu M, Heeger A J, Kim J H, Yoon C O and Lee H 1998 *Adv. Mater.* **10** 456